Theoretical study of multiple-bend quantum wires

Hua Wu and D. W. L. Sprung
Department of Physics and Astronomy, McMaster University, Hamilton, Ontario, Canada L8S 4M1
(Received 26 May 1992; revised manuscript received 25 August 1992)

The electron-transport and bound-state properties of multiple-bend quantum wires, including a ring-type structure, are studied. The emergence of minibands in the low-energy region is well explained in the single-mode approximation.

I. INTRODUCTION

The study of electronic transport properties of the two-dimensional electron gas (2DEG) formed in GaAs-$Al_xGa_{1-x}As$ heterostructures is of great current interest, not only for the basic quantum effects involved but also for the potential engineering applications.[1–5] A narrow constriction is formed by designing gates and applying appropriate electronic potentials on them above the 2DEG. This narrow channel, or quantum wire, then behaves as an electron waveguide due to the high mobility and low scattering probability of electrons in the 2DEG. For simplicity, we adopt a widely used effective-mass approach, in which the electrons, with effective mass m^*, are confined laterally by some potential field. We are interested here in periodic structures defined in the constriction, formed by identical cavities connected serially. Sols *et al.*[6,7] have studied devices of this sort, whereas Brum,[8] and more recently Berggren,[9] have considered a more symmetric configuration, a quantum-dot superlattice. In this paper, we study a quantum wire with many bends, with open or joined ends. For simplicity, the confining potential field is considered to be an infinite square well. The structure is also studied in the one-mode approximation developed in a previous paper.[10] The minibands resulting from the periodic structure[11–13] are easily understood and the one-dimensional nature of the system in the low-energy region is seen clearly.

II. MULTIPLE-BEND QUANTUM WIRE

We study a quantum wire of width d with multiple right-angle bends. The lateral confining potential is assumed to be zero inside and outside to be infinite. Thus the normalized transverse wave function is just $\phi_n(y) = \sqrt{2/d}\sin(n\pi y/d)$ for mode n. The bent wire can be viewed as a series of right-angle bends connected by segments of straight wire of length l. Consider a single unit or cell to consist of one bend with two leads of length $l/2$. For this single unit, the wave functions at the two ends are expanded as

$$\Psi_\Gamma = \sum_n (C_{\Gamma,n}e^{i\alpha_n x} + \bar{C}_{\Gamma,n}e^{-i\alpha_n x})\phi_n(y) \quad , \tag{1}$$

where $\Gamma = 1, 2$ distinguishes the two ends, and

$$\alpha_n = \sqrt{E - \epsilon_n} \tag{2}$$

is the longitudinal wave number associated with the transverse mode n. We express energies $E = k^2$ in units of $\hbar^2/2m^*$. The role of the bend is to relate wave functions at the two ends by a transfer matrix:

$$S_1 = U^{-1}VS_2 \equiv MS_2 \quad ; \tag{3}$$

where

$$S_\Gamma = \begin{pmatrix} C_\Gamma \\ \bar{C}_\Gamma \end{pmatrix} \quad , \tag{4}$$

where C_Γ and $\bar{C}_\Gamma$ are single-column matrices with elements $C_{\Gamma,n}$ and $\bar{C}_{\Gamma,n}$. The forms of U and V can be derived following Ref. 10:

$$U = \begin{pmatrix} (B + i\alpha)P & (B - i\alpha)P^{-1} \\ AP & AP^{-1} \end{pmatrix} \tag{5}$$

and

$$V = \begin{pmatrix} AP^{-1} & AP \\ (B - i\alpha)P^{-1} & (B + i\alpha)P \end{pmatrix} \tag{6}$$

with

$$A_{nn'} = \frac{2nn'\pi^2(-1)^{n+n'}}{d[(n^2 + n'^2)\pi^2 - (kd)^2]} \quad , \tag{7}$$

$$B_{nn'} = \alpha_n \cot(\alpha_n d)\delta_{nn'} \quad , \tag{8}$$

and $P = \exp(i\alpha l/2)$, a diagonal matrix.

Knowing the role of one cell, the properties of the whole wire can be found by means of the total transfer matrix which is the product of all the transfer matrices for the component cells,[14] except for one additional phase F for every two adjacent bends which are bent in opposite directions (as in the case of a double bend forming a staircase):

$$F = \begin{pmatrix} f & 0 \\ 0 & f \end{pmatrix}; \quad f_n = (-1)^{n+1} \quad . \tag{9}$$

While the transfer-matrix method is a simple and powerful approach, it requires the matrix U to be invertible. This will create a numerical problem when many closed channels are to be included in the calculation. An alternative method is to express Eq. (3) as $US_1 = VS_2$,

and apply this to each bend in turn, and to derive a set of linear equations where the wave function on each connecting wire is considered to be an unknown. The method briefly stated here is true for a general periodic structure, however the form of A and B must be adapted for each specific unit-cell structure.

In the low-energy region, one can learn much by considering the single-mode approximation.[10,15,16] By restricting the equations to just to one channel, one reduces U, V, M to 2×2 matrices. Since F is now a unit matrix, the relative bend direction of the adjacent bends makes no difference. It can be shown[17–19] that there is a simple relationship between the transmission probability for a single cell and that for N cells

$$\frac{1}{T_N} = 1 + \frac{|\sin N\phi|^2}{|\sin\phi|^2}\left(\frac{1}{T_1} - 1\right) \quad . \tag{10}$$

Here, ϕ is the Bloch phase for single cell:

$$\cos\phi = \mathrm{Tr}(M)/2 = \frac{B}{A}\cos(\alpha l) - \frac{A^2 - B^2 + \alpha^2}{2\alpha A}\sin(\alpha l) \quad . \tag{11}$$

This relation explains the formation of minibands when N is large: $|\cos\phi| < 1$ induces an allowed band with $N-1$ transparent points, at which $T_N = 1$, which are in addition to those resulting from $T_1 = 1$. On the other hand, $|\cos\phi| > 1$ makes a forbidden band.

The single-bend wire has been discussed in Refs. 20 and 15. The double bend has been calculated by Weisshaar *et al.*[21,13] Their results show that the transmission vs energy curve for a staircase double bend generally follows the single-bend curve but with additional oscillations which can be viewed as representing a standing wave resonance in the middle wire. In Fig. 1 we show the calculated result for a double bend. For the purpose of this paper, we show only the situation where the energy is below the second mode threshold. The dotted curve drawn in the lower part is the exact result. For either direction of the second bend (a U shape or a staircase), one finds the same result in this energy region and thus only one such curve is drawn. The solid curve in the lower part is calculated in the single-mode approximation. The upper part of Fig. 1 shows $\cos\phi$ as defined in Eq. (11). Since N is only two, the forbidden bands are not well developed. We see, however, that each region of $|\cos\phi| > 1$ does produce a minimum. On the other hand, each region where $|\cos\phi| < 1$ gives rise to $N - 1 = 1$ maxima as expected. The maximum value is 1 for each peak (the last one shown does not reach unity due to numerical resolution). For a double bend, Eq. (10) reads $1/T_2 = 1 + 4|\cos\phi|^2(1/T_1 - 1)$. The condition for a maximum is $\cos\phi = 0$. Equation (11) can be rewritten to consist of a positive amplitude function times $\cos(\alpha l + \theta)$ with $\tan\theta = (A^2 - B^2 + \alpha^2)/(2\alpha B)$. The condition for a maximum is then $\alpha l + \theta - \pi/2 = n\pi$. By plotting $\tan(\theta)$, we find θ changes from $\pi/2$ to about 2π in the region $\pi/d < k < 2\pi/d$. We see immediately that when l is large, the maximum condition is that αl be an integer multiple of π. This is why the maxima can be viewed as standing waves in the middle connecting wire. Furthermore, the number of maxima in a given interval is given by the integer part of $\sqrt{3}l + 1.5$. For the situation illustrated in Fig. 1, $l = 4$ and there are eight maxima.

Next we discuss results for a ten-bend wire. There are many possible configurations with ten bends. In the inset of Fig. 5 we show two of these configurations, which we call (a) staircase and (b) corrugated shape. Figure 2 shows exact calculations for these two configurations. As expected, the transmission probabilities for the two configurations are very similar in the plotted region,

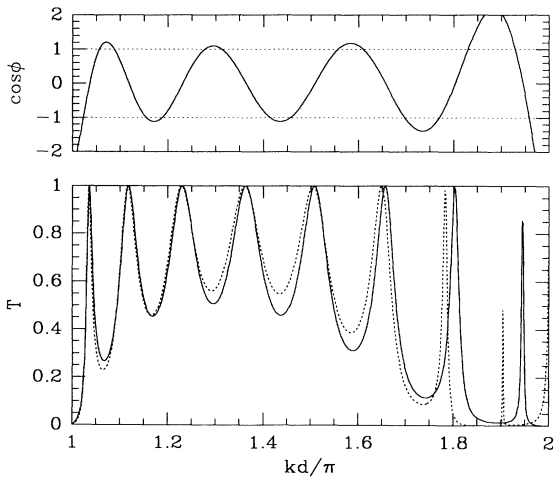

FIG. 1. Transmission probability for a double bend. $l = 4d$. Upper part: cosine of Bloch phase of the double bend. Lower part: the dotted curve is the result with the single-mode approximation, whereas the solid line is the exact calculation.

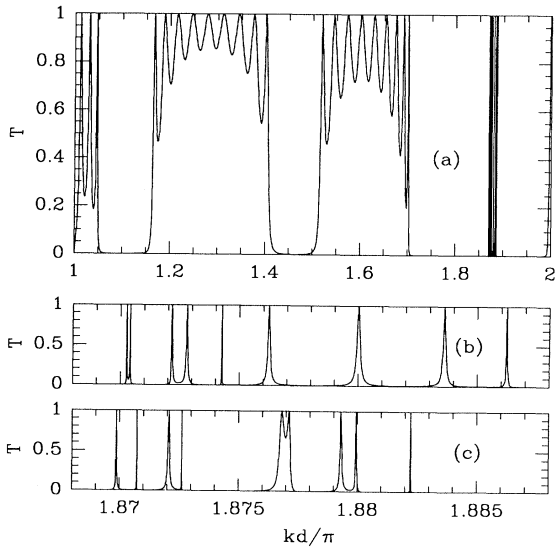

FIG. 2. Exact calculation for ten-bend wires with $l = d$. (a) Transmission probability for the staircase shape, with energy running from the first-mode threshold to the second-mode threshold. The result for the corrugated shape is very similar. In (b) and (c), the third allowed zone is expanded. (b) is for the staircase and (c) is for the corrugated shape.

thus only the curve for the staircase shape is shown in Fig. 2(a). There are three complete allowed zones, and each has exactly nine maxima. The first allowed zone is not complete; there are only three peaks. This is because the variation of the Bloch phase in this zone is less than π, as seen in the upper part of Fig. 2. In order to see the difference between the two configurations, we expand the third complete allowed zone. Figure 2(b) is for the staircase shape; Fig. 2(c) is for the corrugated shape.

The single-mode approximation result is shown in Fig. 3. As in Fig. 2, the upper part is the cosine of the Bloch phase. In the lower part there are three curves. The solid one is the transmission probability. We see that both allowed and forbidden bands are well developed. Compared to Fig. 2, though not identical, it is remarkably similar. The dotted curve is the envelope function for the minima of the allowed bands. It is derived from Eq. (10) by setting $|\sin N\phi| = 0$. The dashed curve is T_1, the transmission probability for a single bend in the single-mode approximation. As can be predicted from Eq. (10), it passes through the center of each allowed band envelope function. It is clearly seen that in the low-energy region, the periodic quantum wire is dominated by its one-dimensional nature.

Figure 4 shows the conductance of a ten-bend wire in the staircase shape with $l = d$. The upper part of Fig. 4 are the cosines of the Bloch phase calculated exactly by solving the generalized eigenvalue problem

$$U\psi = e^{i\phi}VF\psi \quad , \tag{12}$$

where F is needed to account for the extra phase from opposite direction bends. It can be shown that $\pm\phi$ always appear together as conjugate solutions; each pair of real ϕ represents one channel which allows electrons to propagate. In Fig. 4 we plot $\cos\phi$, but only for those points with real ϕ values. The part of the curve from $kd/\pi = 1$ to 2 is identical to Fig. 2, where there is only one pair of ϕ (except a very narrow region around $kd/\pi = 1.8$). From $kd/\pi = 2$ to 3, we still see some well-developed minibands. This can be explained by the fact that basically there is only one pair of ϕ for a given k value, and thus just one channel. In this case, the mechanism of formation of the miniband is the same as in the single-mode approximation. However, if there are two pairs of ϕ in a region, we see peaks reaching up to $G = 2$. This argument applies equally to the higher energy region. It is observed that the conductance is greatly reduced by the bends in the wire as compared to the straight wire. The result for a corrugated wire is similar though there are noticeable differences beyond the second mode.

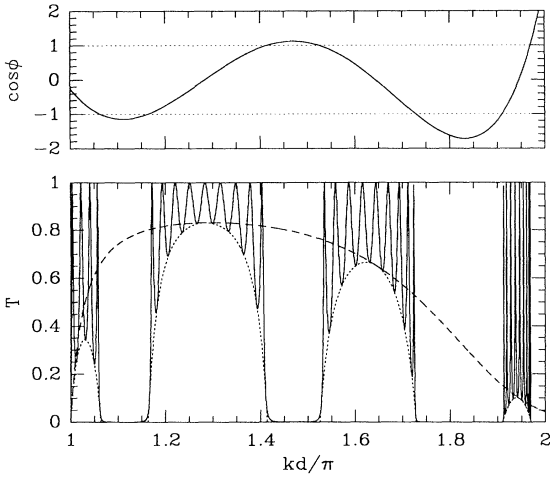

FIG. 3. Single-mode approximation for a ten-bend wire as shown in Fig. 2. Upper part: the cosine of Bloch phase. Lower part: solid line, the transmission probability T_{10}; dotted line, the predicted envelope function of the minima; and the dashed line, transmission probability for a single bend T_1 in the single-mode approximation.

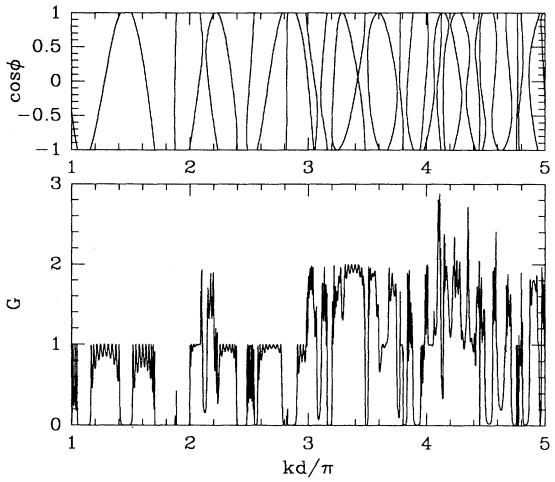

FIG. 4. Conductance of the ten-bend staircase shape wire in units of $2e^2/h$. $l = d$. The conductance is shown in the lower part, while the cosines of the Bloch phases are shown in the upper part. Only those points with real ϕ value are plotted.

Following the work of Schult, Ravenhall, and Wyld,[22] it is known that junctions and open quantum dots can support bound states. Their properties have been discussed in the literature, in particular, their possible detection as tunneling resonances.[7,9,15,20,23,24] The bound state for a single bend lies at $E = 0.929\epsilon_1$.[20,15] For a multiple-bend wire, there may be more than one bound state. In general, each bend should support one. When the interbend distance is large, these states are decoupled, and thus we have N degenerate states. When the distance l is shortened, interaction between these states removes the degeneracy and produces a miniband. Some levels are pushed up while others are pushed down. Since only those states below ϵ_1 are bound, some states may disappear when l is less than a threshold value. The situation can be well understood by modeling it as a multisquare-well problem in one dimension.[10] In this picture, the widest well occurs at $l = 0$, when the system has its lowest bound state. In Fig. 5 we plot the bound states for the two types of bent wire as shown in the inset of Fig. 5. It is seen that the bend direction makes little difference. The convergence to the single-bend bound-state energy is seen clearly as l increases.

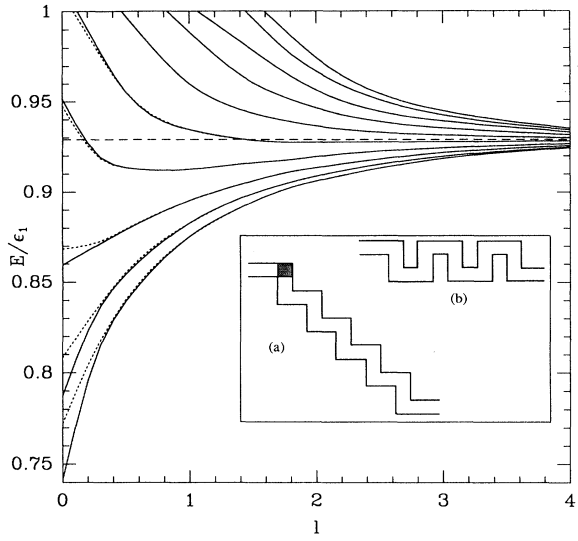

FIG. 5. Bound-state energies for a ten-bend wire with open ends. Solid line: the corrugated shape. Dotted line: the staircase shape. Dashed line: mark for the single-bend bound-state energy. The inset shows the two particular ten-bend wire configurations; $l = d$. (a) The staircase shape and (b) the corrugated shape.

III. ARTIFICIAL CRYSTAL MADE FROM BENT WIRE

In the previous section, we have focused our attention on the transmission problem. We assumed that the system was open: electrons enter the structure from one end and leave it from the other. The bound states, if any, were those corresponding to an electron trapped in the structure with energy less than the propagating threshold. In this section we will discuss instead closed systems consisting of serially connected identical cells. This closing is done by joining the beginning and end of the chain. In such a structure, periodic boundary conditions arise naturally. However, unlike the usual solid-state crystal, only a finite number of cells are involved.

For an artificial crystal made from bent wire, there are many possible configurations, depending on the number of bends. The simplest is the square four-bend crystal. The next possibility is a 12-bend structure forming a cross as in the inset of Fig. 7. Strictly speaking, the basic cell for this cross consists of two left- and one right-handed bend. However, as we have seen in the last section, the bending direction makes no difference if the energy is below the second threshold. Thus we will treat the cross as a 12-cell crystal.

Due to its geometrical symmetry,

$$S_{j+1} = e^{i\phi} S_j \quad , \tag{13}$$

where ϕ is a solution of a generalized eigenvalue problem:

$$U\psi = e^{i\phi} V\psi. \tag{14}$$

In the single-mode approximation this definition is identical to that of the Bloch phase introduced in Eq. (11). However, now ϕ is quantized: since the system is closed: $S_{N+1} = S_1$, and thus

$$\phi = 2\pi m/N, \quad m = 0, 1, ..., N-1 \quad . \tag{15}$$

Figure 6 shows the spectrum of the four-bend crystal for energy below $4(\pi/d)^2$, which would be the second propagating mode threshold. The left half of the figure is the result of the single-mode approximation while the right half is from an exact calculation. For the four-bend crystal, allowed states exist for $\phi = 0, \pm\pi/2$, and π. States with $\phi = \pm\pi/2$ are degenerate. We wish to discuss in detail the first four states, which have a direct connection to the bound state found for an open single-bend wire at energy $0.929\epsilon_1$.[20,15] If l were very large, the four states would be degenerate at this energy. The situation is similar to the double-bend wire discussed in Ref. 10. The four states have definite symmetries associated with ϕ. If we label the four bends as 1,2,3,4 and represent the wave function at the first bend with a +1 symbol, the four states will show the following patterns:

ϕ	Pattern
0	+1 +1 +1 +1
$\pi/2$	+1 $+i$ −1 $-i$
$-\pi/2$	+1 $-i$ −1 $+i$
π	+1 −1 +1 −1

Since states with $\phi = \pm\pi/2$ are degenerate, one can combine them to make real wave functions having the pattern $+1, 0, -1, 0$ and the 90° rotation of $0, +1, 0, -1$. When l is decreased, the ground state being most symmetric is lowered in energy by spreading of the wave function into the connecting links, while the other states rise

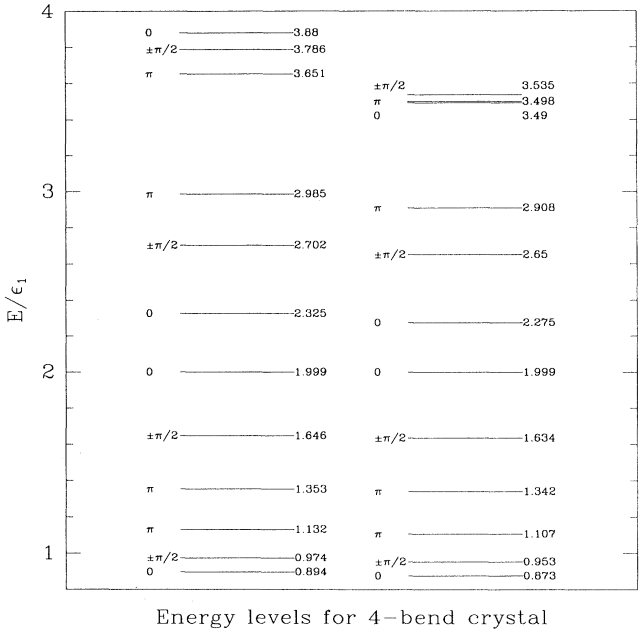

FIG. 6. Spectrum for the four-bend crystal. On the left are results from the single-mode approximation and on the right are exact results. Energies are expressed in terms of the first propagating threshold energy $\epsilon_1 = (\pi/d)^2$. The label to the left of each level is the associated ϕ value. States with $\phi = \pm\pi/2$ are degenerate.

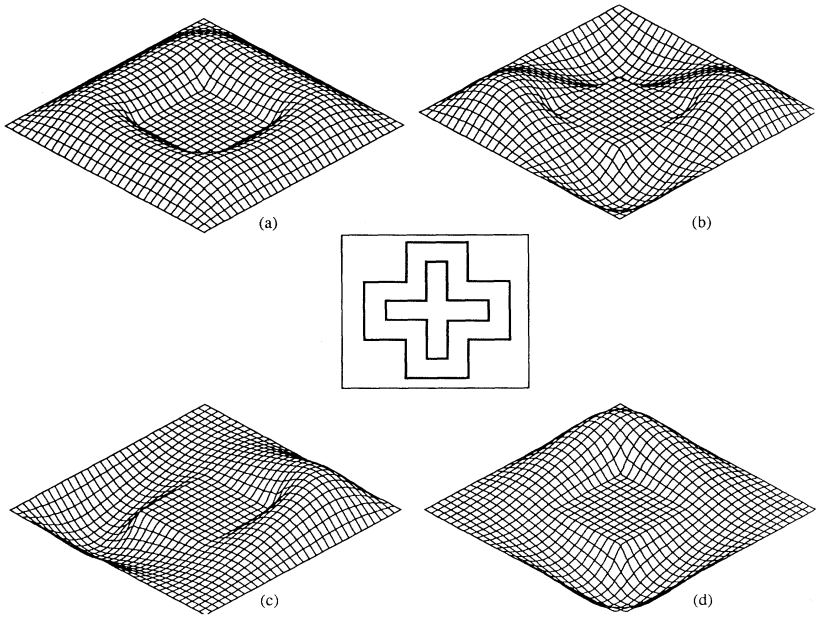

FIG. 7. Wave functions for the first four states of the four-bend crystal. (a) $\phi = 0$, the ground state; (b) $\phi = \pi$, the fourth state. (c) and (d) Real wave functions for $\phi = \pm\pi/2$ states. The inset in the center is an artificial cross-shape crystal made of 12 bends.

in energy because their symmetries force the wave function to be squeezed into the bend region. Figure 7 shows the wave functions for these four states.

The cross-shaped crystal with 12 bends is the simplest possible beyond the four-bend square crystal. Just as we described its states by the quartet of values taken by the wave function on the four sites, here we require a 12-plet. Four of the states are just the threefold repetition of the previous quartets; these states have the same ϕ value and the same phase change between adjacent sites, hence the same energy. All the states can be described by wave functions of the pattern

$$\cos\frac{2\pi n_s}{n}x_b, \quad x_b = 1, ..., 12 \tag{16}$$

or

$$\sin\frac{2\pi n_s}{n}x_b, \quad x_b = 1, ..., 12 \tag{17}$$

where $n_s = 0, 1, ..., n/2$ labels the states and x_b labels the bend sites. The values $n_s = 1, n/2$ give the purely symmetric $[(+1)^{12}]$ and antisymmetric $[(+1, -1)^6]$ states, associated only with the cosine, while the other values give two degenerate states associated with the sine and the cosine. (To distinguish the degenerate states, one could use labels $1c$ and $1s$, etc.) The degeneracies and energies of the first 12 bound states in terms of ϵ_1 are 1×0.874, 2×0.883, 2×0.909, 2×0.953, 2×1.010, 2×1.073, and 1×1.108.

IV. CONCLUSION

We have studied a particular periodic quantum wire structure formed by multiple right-angle bends. This particularly simple configuration shows how the minibands develop in a finite periodic system. We have also analyzed the system in the single-mode approximation. These analytic results agree well with the exact calculations, and demonstrate that the system is dominated in the low-energy region by its underlying one-dimensional nature.

ACKNOWLEDGMENTS

We are grateful to NSERC Canada for continuing support under research Grant No. OGP-3198. We also thank Professor J. Martorell for fruitful discussions. D.W.L.S. is grateful to the Spanish Ministry of Education and Science (DGICYT).

[1]C. W. Beenakker and H. Van Houten, Solid State Phys. **44**, 1 (1991).
[2]G. Bastard, J. A. Brum, and R. Ferreira, Solid State Phys. **44**, 229 (1991).
[3]Phys. Today **43** (2), 22 (1990).
[4]S. Datta, Superlatt. Microstruct. **6**, 83 (1989).
[5]Phys. World **5** (3), 50 (1992).
[6]F. Sols, M. Macucci, U. Ravaioli, and Karl Hess, Appl. Phys. Lett. **54**, 350 (1989).
[7]F. Sols, M. Macucci, U. Ravaioli, and K. Hess, J. Appl. Phys. **66**, 3892 (1989).
[8]J. A. Brum, Phys. Rev. B **43**, 12 082 (1991).
[9]Zhen-Li Ji and K.-F. Berggren, Phys. Rev. B **45**, 6652 (1992).
[10]Hua Wu, D. W. L. Sprung, and J. Martorell, Phys. Rev. B **45**, 11 960 (1992).

[11]L. P. van Kouwenhoven, F. W. J. Hekking, B. J. van Wees, C. J. P. M. Harmans, C. E. Timmering, and C. T. Foxon, Phys. Rev. Lett. **65**, 361 (1990).
[12]S. E. Ulloa, E. Castaño, and G. Kirczenow, Phys. Rev. B **41**, 12 350 (1990).
[13]A. Weisshaar, J. Lary, S. M. Goodnick, and V. K. Tripathi, J. Appl. Phys. **70**, 335 (1991).
[14]Hua Wu, D. W. L. Sprung, J. Martorell, and S. Klarsfeld, Phys. Rev. B **44**, 6351 (1991).
[15]J. Martorell, S. Klarsfeld, D. W. L. Sprung, and Hua Wu, Solid State Commun. **78**, 13 (1991).
[16]D. W. Sprung, Hua Wu, and J. Martorell, J. Appl. Phys. **71**, 515 (1992).
[17]D. J. Vezzetti and M. Cahay, J. Phys. D **19**, L53 (1986).
[18]M. Cahay and S. Bandyopadhyay, Phys. Rev. B **42**, 5100 (1990).
[19]D. W. L. Sprung, Hua Wu, and J. Martorell (unpublished).
[20]P. Exner, P. Šeba, and P. Štoviček, Czech. J. Phys. B **39**, 1181 (1989).
[21]A. Weisshaar, J. Lary, S. M. Goodnick, and V. K. Tripathi, Appl. Phys. Lett. **55**, 2114 (1989).
[22]R. L. Schult, D. G. Ravenhall, and H. W. Wyld, Phys. Rev. B **39**, 5476 (1989).
[23]K.-F. Berggren and Zhen-li Ji, Superlatt. Microstruct. **8**, 59 (1990).
[24]K.-F. Berggren and Zhen-li Ji, Phys. Rev. B **43**, 4760 (1991).